Detection and Reconstruction of Human Scale Features from High Resolution Interferometric SAR Data

R. Bolter, Graz University of Technology, Austria

ICPR 2000, Barcelona

Abstract

In contrast to opical imagery, modern high resolution IFSAR sensors deliver intensity images and corresponding interferometric height and coherence data from a single flight path at pixel sizes of 30cm to 10cm. Due to the all-weather, day-night applicability of SAR sensors, multiple views over a short time can be easily obtained. However, many image users find it difficult to "read" radar images. They differ from the natural human visual impression and the familiar analogy communicated by optical imagery. The goal of our work is to convert radar data into models of the terrain and render those models in analogy to the optical sensing approach that the human visual system represents. Therefore intelligent combinations of multiple views and measurements from all IFSAR data sources available are necessary to help to overcome problems inherent in the SAR data as e.g., blur, speckle, layover, and shadow. Using basic image analysis methods we present in this paper our first fully automated approach to separate buildings from other objects in an IFSAR dataset. The building shapes are reconstructed using a simple building model and the results are compared to measurements made from optical imagery.

1. Introduction

High resolution SAR imagery has begun to get consideration as a source for detection and reconstruction of human scale features [1]. Airborne sensors deliver high resolutions at pixel sizes of 30cm to 10cm and single pass interferometry supports the geometric reconstruction of various human scale features. Interferometrically derived digital elevation models are usually less detailed than the basic magnitude images and suffer from effects of image blur, speckle, layover, and shadows. However, due to the all-weather, day-night capability of SAR sensors it is possible to image any region multiple times over a short period.

Extraction of man-made objects from optical imagery is a lively topic in the remote sensing community, e.g., [3] and [5]. Previous demonstrations of such measurements from SAR data were based on manual work, some limited automated methods can be found. In [6] fusion of IFSAR and multispectral optical image data results in boundary boxes of buildings. [4] describes an automated region growing approach to localize buildings starting from the shadows they cast. The reconstruction of building shapes of urban tower blocks from IFSAR data by applying a range segmentation algorithm is presented in [2]. Another approach to enhance the quality of IFSAR imagery is described in [1]. In contrast to these previous demonstrations, which are performed on a single data source we want to employ the best source for each single measurement and combine the results in an intelligent way.

2. Test Data

In this paper we will focus on the detection and reconstruction of buildings at the McKenna MOUT site, Ft.Benning, GA. The buildings on this site are clustered in a compact group resembling a northern European village, surrounded by undeveloped land. Figure 1 shows an optical image of the test site. From an airborne Sandia Spotlight IFSAR sensor the testsite was imaged from four cardinal azimuth directions. Each pass was processed into four channels: magnitude, correlation, height and bin number, and converted to UTM coordinates. The original slant range magnitude images are also available.

An ARC/INFO data set of the Fort Benning MOUT site is used as the ground truth to evaluate the building extraction results. This data set contains the UTM coordinates of building corners, building areas, perimeters as well as building heights, etc.

3 Methods

To simplify the radar interpretation process, our first goal is to separate the buildings from the other objects in the imaged scene, e.g. trees, bushes, streets, grassland. As stated previously, each single data source is disturbed by speckle noise and in case of the steep slopes of buildings and trees

Figure 1. Optical image of the Ft. Benning MOUT testiste

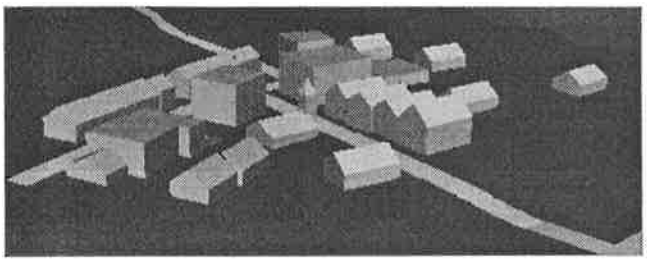

Figure 2. Shaded view of ground truth.

especially by layover and shadow effects. These effects depend direct on the illumination direction, therefore a combination of the information gained from the four cardinal azimuth directions might help.

For the interferometric height data, shadow results in an area of no values facing away from the backslope of an object, and layover results in the so called "front porch" anomaly [1]. This effect appears as an extended region on the near-range side of an object that is characterized by altitudes in between the values on the ground and the values at the objects top. So both effects result in lower height values than expected at particular view dependent areas in the image.

Figure 3 shows from left to right four independents views of interferometric height data of two individual buildings from our testsite. The view dependence of layover and shadow effects can be seen. For the combination of these four independent views we used a simple maximum decision strategy, for each pixel in the scene, the maximum height value over all four measurements was chosen. Although due to the front porch effect this may result in larger building areas than actually given, this strategy makes the detection of even small buildings possible. The resulting fused height image of these two buildings can be seen from the righthandside of figure 3. This combined height measurements are still quite noisy, therefore a 3-by-3 median filter was applied after the maximum combination step.

From this enhanced height image a decision between bare earth and objects rising up from these bare earth can

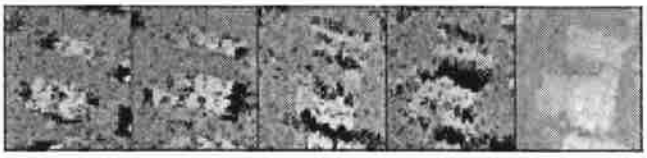

Figure 3. From left to right: interferometric height data for two buildings from four independent views and maximum combination of these four views.

be drawn easily. A large area minimum filter was applied to extract the bare earth. The window width of the filter was larger than the largest object in the scene, in our case this was 15 by 15 pixels. Every pixel in the filtered image was assigned the minimum value from the surrounding window. Subtracting the resulting bare earth from the original height measures and applying a single threshold delivered a binary mask, where all objects rising up from the bare earth by more than the threshold were selected.

From these binary masks it is possible to calculate startpoints for regions of interest where buildings are supposed to be. Therefore several morphological erosions were applied to the binary mask. The resulting regions were labeled, and all regions exceeding a certain number of pixels were considered for further exploitation. The next step was to blow up these startregions to their original size and shape. Therefore the same number of morphological operations as before was performed on the startregion, but this time the dilation operator was used and the resulting region was intersected with the original mask. Because in this first approach, we just want to fit simple building models, minimum bounding rectangles over the selected regions were calculated.

The differentiation between buildings and other objects rising up from the bare earth, e.g. trees, bushes, can not be drawn from the height measurements alone. Therefore during the height measurement combination step a corresponding combined coherency map was computed. For each position in the map, the coherency value corresponding to the selected height value was chosen. Texture measures were calculated in the selected region from the coherency and height information. Mean and standard deviation of the coherency and height data first among the selected points and than over the whole minimum bounding rectangle were calculated. From these measurements a decision between buildings and other objects was possible. The mean coherency for buildings is usually superior to the vegetation mean coherency, the standard deviation of the height values is usually lower than for the vegetation, if calculated just on the segmented points. Due to the steep slopes of buildings the standard deviation of the height values for buildings

Figure 4. IFSAR segmentation result.

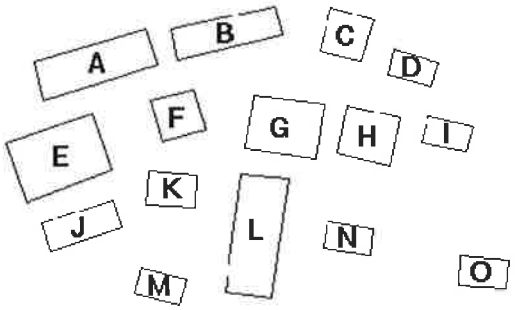

Figure 5. Building's footprints with assigned letters corresponding to the ground truth data.

increases significantly if calculated over the whole minimum bounding rectangle, compared to vegetation. Figure 4 shows the result of this simple segmentation process into three classes, bare earth, trees and buildings.

To enhance the information content of the result for the IFSAR image user we tried to fit simple building models over the segmented building areas. The two most simple building models are flat roofed and symmetric gable roofed. Therefore we used all selected points within the minimum bounding rectangle and calculated a least squares plane fit. Then the minimum bounding rectangle was split up in the middle and planes were fit to each half, this was done for both directions of the rectangle. The quadratic errors between actual height data and fitted plane were calculated for all planes, and the model with the overall minimum error was chosen. A shaded view of the resulting buildings can be seen from figure 6.

4 Results

Ground truth data for the building models is available for the testsite. Figure 5 shows the footprints of the buildings extracted manually from the optical imagery. The corresponding footprints of the buildings extracted automatically with our method from the IFSAR data can be seen from the segmented image in Figure 4. In Table 1 the resulting centroid values of the buildings in offsets to UTM coordinates are compared to the ground truth measurements. Table 2 gives the resulting area and height measurements of our method and the corresponding ground truth data and resulting errors.

5 Discussion

The described segmentation method works quite well for the given dataset, although discrimination in just three classes will be not sufficient for some applications. The extracted building centers correspond quite well to the ground truth data, as can be seen from Table 1. The mean error is 1.93 m. The extracted areas, on the other hand, differ significantly from the actual buildings areas, as can be seen from Table 2. Small buildings are underestimated, larger buildings are overestimated. This is obviously a problem of the segmentation procedure of the noisy height measurements. Enhancements should be possible, by incorporating not just the height and coherence measurements but also the original slant range magnitude SAR images of the four independent views. Therefore the information from the slant range images has to be transformed to UTM coordinates.

The model fitting procedure delivered satisfactory results, too, as can be seen from the shaded view of the extracted buildings from Figure 6. The mean error for the maximum height of the extracted buildings lies below 1 meter, if the maximum error for the church (k) is excluded. The steeple of the church can not be covered by our simple models, the resulting gable roof for the church is tilted towards the steeple, as can be seen from the shaded view in Figure 6. One other building (L) corresponds not to our simple models, apart from these two exceptions just one building (F) was assigned a wrong model, a gable roof instead of a flat roof. So within the limits of the available three simple building models (flat roofed, gable roofed in two directions) the results are quite promising, especially because no manual interaction was needed during the extraction procedure.

Bldg.	Cent. X		Cent. Y		
	optical	IFSAR	optical	IFSAR	error
A	489.983	491.681	621.318	621.290	1.70
B	526.127	526.834	629.862	628.605	1.44
C	559.093	557.518	629.054	625.121	4.24
D	577.152	580.073	619.899	618.242	3.36
E	479.750	479.692	595.179	598.735	3.56
F	512.775	513.017	606.923	606.457	0.53
G	542.010	543.903	603.641	603.815	1.90
H	565.001	565.239	601.150	600.157	1.02
I	586.376	586.778	601.554	599.751	1.85
J	486.183	487.617	576.224	576.383	1.44
K	510.991	512.204	586.255	586.746	1.31
L	534.218	534.759	573.632	572.319	1.42
M	507.844	506.921	559.444	557.485	2.16
N	559.497	560.362	572.521	572.319	0.89
O	596.087	597.345	563.282	561.549	2.14

Table 1. Extracted buildings center coordinates in offsets to UTM and the corresponding error in meters.

Bldg.	Area			Hgt.		
	optical	SAR	error	opt.	SAR	err.
A	349.9	541.1	+191.1	8.8	7.9	-0.9
B	259.1	370.0	+110.9	8.9	10.0	+1.1
C	149.4	244.8	+95.4	7.4	7.0	-0.4
D	88.4	59.5	-28.9	6.2	6.9	+0.7
E	439.3	558.6	+119.3	7.0	6.0	-1.0
F	147.4	277.5	+130.1	7.4	7.6	+0.2
G	297.1	535.8	+238.7	11.0	9.2	-1.8
H	201.9	230.0	+28.1	3.7	4.3	+0.6
I	90.4	56.3	-34.1	6.2	6.4	+0.2
J	166.1	206.1	+40.0	6.1	4.1	-2.0
K	117.6	160.5	+42.9	12.1	7.5	-4.6
L	426.9	589.5	+162.6	9.4	10.2	+0.8
M	92.9	55.8	-37.1	6.1	5.2	-0.9
N	94.1	75.3	-18.8	6.1	5.1	-1.0
O	102.5	123.4	+20.9	6.1	4.8	-1.3

Table 2. Extracted buildings area and height measurements compared to ground truth data. The building areas are given in square meters, the height data in meters.

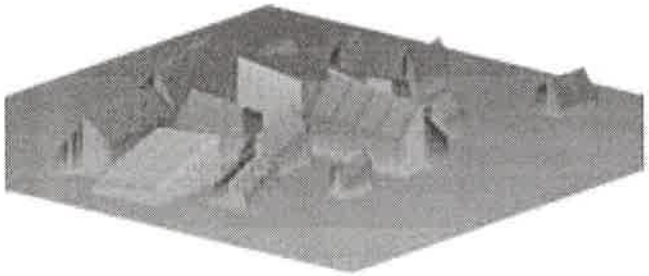

Figure 6. Shaded view of extracted buildings.

6 Summary and Outlook

In this paper we have presented our first fully automated approach to building extraction from multiple view interferometric SAR datasets. By an intelligent combination of the different measurements available and applications of standard image analysis methods, a coarse segmentation into three classes was possible. To split this classification into more classes, the incorporation of original slant range magnitude images will be necessary.

The extracted building models fit quite well to the actual buildings, apart from the estimated building areas. Incorporation of original slant range magnitude images should help in this case as well. The building's back walls are defined quite good in the slant range images by the shadows they cast, combining the shadow-edges from four independent views should give a better hint of the actual building dimensions. More complex building models should be incorporated by splitting the selected building areas into further planes.

Acknowledgements

We wish to thank Bob Wilson from Vexcel Corporation, Boulder, for providing the data.

References

[1] G. Burkhart, Z. Bergen, and R. Carande. Elevation correction and building extraction from interferometric sar imagery. In *Proceedings of IGARSS'96*, pages 659–661, 1996.

[2] P. Gamba and B. Houshmand. Three dimensional urban characterization by ifsar measurements. In *Proceedings of IGARSS'99*, 1999.

[3] A. Gruen, O. Kuebler, and P. Agouris, editors. *Automatic Extraction of Man-Made Objects from Aerial and Space Images*. Birkhäuser Verlag, 1995.

[4] K. Hoepfner, A. Hanson, and E. Riseman. Recovery of building structure from sar and ifsar images. In *ARPA Image Understanding Workshop*, pages 559–563, 1998.

[5] F. Leberl, R. Kalliany, and M. Gruber, editors. *Mapping Buildings, Roads and other Man-Made Structures from Images*. Proceedings of the IAPR TC-7 Workshop "Remote Sensing and Mapping", R. Oldenburg, Wien, 1997.

[6] R. Xiao, C. Lesher, and B. Wilson. Building detection and localization using a fusion of interferometric synthetic aperture radar and multispectral image. In *ARPA Image Understanding Workshop*, pages 583–588, 1998.